Effects of the Size and Filler Loading on the Properties of Copper- and Silver-Nanoparticle-Filled Epoxy Composites

K. L. Chan,[1] M. Mariatti,[1] Z. Lockman,[1] L. C. Sim[2]

[1]*School of Material and Mineral Resources Engineering, University Sains Malaysia, Engineering Campus, 14300 Nibong Tebal, Penang*
[2]*Intel Technology (Malaysia) Sendirian Berhad, Penang, Malaysia*

Received 5 March 2010; accepted 21 November 2010
DOI 10.1002/app.33798
Published online 6 April 2011 in Wiley Online Library (wileyonlinelibrary.com).

ABSTRACT: Copper-nanoparticle (CuNP)-filled nanocomposites were prepared with various particle sizes and loadings. The nanocomposites incorporating 20-nm CuNPs with 5 vol % loading displayed optimum properties as determined by electrical, mechanical, and thermal characterization. Silver nanoparticles (AgNPs) with a size of 20 nm were loaded into the epoxy resin to allow a comparison of the properties. Interestingly, at the percolation threshold, a 5 vol % loading of CuNP and AgNP nanocomposites resulted in slightly similar electrical conductivities of 0.01 and 0.02 S/cm, respectively. The CuNP and AgNP nanocomposites were also subjected to thermal aging at 150°C, and we observed that the electrical conductivity of both nanocomposites dropped only by about one order of magnitude after 8 weeks of exposure. © 2011 Wiley Periodicals, Inc. J Appl Polym Sci 121: 3145–3152, 2011

Key words: composites; electron microscopy; fillers; mechanical properties; thermal properties

INTRODUCTION

For decades, tin/lead (Sn/Pb) has been the material of choice as an interconnecting material in electronic packaging because of its good electrical conductivity, economical cost, and ease of application during part assembly.[1–3] However, upon disposal, the presence of Pb in electronic packaging has adverse effects on both human beings and the environment. To overcome this issue, the development of electrically conductive adhesives (ECAs) has gained attention in the electronics sector as an alternative material for the replacement of lead in electronic part interconnections.[1,3] ECAs are polymer composites comprised of a polymer matrix and electrically conductive fillers. ECAs also offer an additional advantages over conventional Sn/Pb solders, such as a lower processing temperature, finer pitch, and lower cost.[1,4] ECAs serve as a two-surface binder and provide continuously conductive electrical paths that allow electrons or charges to be transferred simultaneously. The ECA filler is usually selected from high-electrical metal conductive substances, such as gold, silver, copper, and nickel. The selection of the type of metal filler is equally as crucial as the matrix selection because the filler may provide a reinforcing effect on the ECA mechanical properties because of a higher hardness and modulus of elasticity compared to the polymer matrix.[3,5–7]

Currently, ECAs in electronic packaging consist mainly of the application of microflaked silver filler as the conductive agent in an epoxy matrix. In that formulation, a high filler loading of the microflaked silver is required for incorporation into the epoxy matrix before the electrical percolation threshold is reached. Normally, the threshold occurs when microflaked silver filler is loaded at approximately 80 wt %.[3] A high filler loading for an ECA is not economical and aggravates the issue of natural resource (metal) consumption. With the advancements in nanotechnology, much smaller metal nanoparticles can be synthesized. Nanoparticles, with a high specific area, are a huge advantage in applications with ECAs because they create a higher contact area among the surfaces at the same filler loading. Thus, the electrical percolation threshold is theoretically achievable at much lower filler loadings, and this was proven in our previous study,[2] where the percolation threshold was achieved at approximately 40 wt %. However, the incorporation of metal nanoparticles does not promise better properties in ECAs. Poor composite preparation will lead to agglomeration and sedimentation of the nanoparticles; this

Correspondence to: M. Mariatti (mariatti@eng.usm.my).
Contract grant sponsor: Intel Technology (M) Bhd. student scholarship granted to K. L. Chan.
Contract grant sponsor: Ministry of Higher Education of Malaysia and University Sains Malaysia; contract grant number: 1001/PBAHAN/814055.

© 2011 Wiley Periodicals, Inc.

causes detrimental effects, especially to the electrical conductivity of the ECA. To understand and prevent agglomeration and sedimentation of the nanoparticles, many studies have been carried out,[2,8,9] and it has been discovered that solvent ultrasonication is the best method for the breakdown and dispersion of nanoparticles before introduction into the epoxy matrix. To the best of our knowledge, few studies of the properties of copper-nanoparticle (CuNP)-filled epoxy composites have been done. CuNPs have been known as oxidation-sensitive metal substances; thus, it has been reported that the electrical conductivities of the CuNP-filled epoxy composites will decrease after composite fabrication because of the oxidation process.[1,3]

Previous studies[1–3] have been generally focused on silver as a filler for ECA applications; this is because of silver's higher electrical conductivity, which is approximately 6.5×10^5 S/cm. In view of the similar electrical conductivity (5.9×10^5 S/cm) and low cost of copper, we carried out this study to characterize the properties of various sizes of CuNPs in epoxy composites and compared them with the properties of silver-nanoparticle (AgNP)-filled epoxy composites.

EXPERIMENTAL

Materials

In this study, epoxy (EPON 8281) with the chemical name bisphenol A epichlorohydrin was selected as the polymer matrix. The resin was supplied by Hexion Specialty Chemical Sendirian Berhad (Kuala Lumpur, Malaysia). The curing agent for EPON 8281 was polyetheramine (PEA) D230, which was supplied by BASF Corp. CuNPs and AgNPs were purchased from Xuzhou Hongwu Nanometer Material Co., Ltd. (Guangzhou, China) Nanostructured & Amorphous Materials Inc. (Houston, Texas) respectively. The sizes of the CuNPs were 100, 50, and 20 nm, whereas the size of the AgNPs was 20 nm.

Preparation of the ECA

The ECA had a density of 1.18 g/mL at 298 K and was fabricated with a mixing ratio of 100 : 32 for EPON 8281 to PEA. The amounts of CuNPs or AgNPs (20 nm) necessary for incorporation in the epoxy matrix at various loadings of 1, 3, 5, and 7 vol % were measured; a 95% chloroform solution was added at excess (a ratio of 1 : 3) and then ultrasonicated in a bath at room temperature (30°C) for 20 min. After the sonication process, the chloroform nanoparticle solution was dried in a vacuum oven at −1 atm and 80°C for approximately 45 min. The dried nanoparticles were introduced into the EPON 8281 and stirred with a homogenizer at 20,000 rpm for 15 min. PEA was added to the epoxy–nanoparticle paste and homogenized again for an additional minute to improve the distribution of PEA in the epoxy. Lastly, the stirred paste was sent for precuring at −1 atm in a vacuum oven for 1 h; this was followed by postcuring at 125°C for 3 h. This ECA preparation technique was repeated for the fabrication of ECAs loaded with filler sizes of 20 and 50 nm. For the aging study, samples of ECA loaded with 5 vol % of 20-nm CuNPs and AgNPs were exposed to a temperature of 150°C in an air oven and aged for 8 weeks.

Characterization

The morphological properties of the produced ECA were studied with field emission scanning electron microscopy (FESEM) and light microscopy (LM). A Zeiss SUPRA 35VP FESEM (Oberkochen, Germany) instrument equipped with a Gemini field emission column was used. Backscattered electron mode was selected to study the ECA morphology because of the advantage of better image contrast in this mode. Before FESEM scanning, the fractured ECA sample was coated with gold for the purpose of preventing electron buildup on the epoxy matrix surface during scanning. To intensively study the morphology of the ECA, it was necessary to acquire a nanoparticle distribution overview. Thus, microtome sectioning was performed on the ECA, with a film thickness of 1 μm. The microtome was sent for viewing under LM at a magnification of 825×. An Olympus BX51 light microscope fitted with a Sony Exware HAD color digital video camera was used to capture images, and the distribution of nanoparticles in the epoxy matrix was analyzed with an Image Pro Express Version 4.0 image analysis system. Philips CM 12 transmission electron microscope (Amsterdam, The Netherlands) equipped with a Docu Version 3.2 image analysis system was used in this study. An Instek LCR-817 instrument was used to measure the electrical properties of the ECA with a voltage of 1 V supplied through the electrical probe and the ECA. The value of the electrical resistance was measured after 30 s of steady current flow through the ECA samples. For the ECA mechanical property measurements, the ECA was subjected to a three-point bending test according to ASTM D 790-98, for which a rectangular ECA sample with dimensions $100 \times 13 \times 2.5$ mm^3 was prepared. The span length was set at 40 mm with an overhang of 30 mm at each end. The crosshead speed was set at a constant speed of 5 mm/min. The coefficient of thermal expansion (CTE) of ECA was acquired with a Linseis L75/1550 dilatometer (Selb, Germany). The dimensions of the ECA sample were $50 \times 4 \times 4$ mm^3, and the sample was exposed to test temperatures of 30–200°C at a heating rate of 3°C/min.

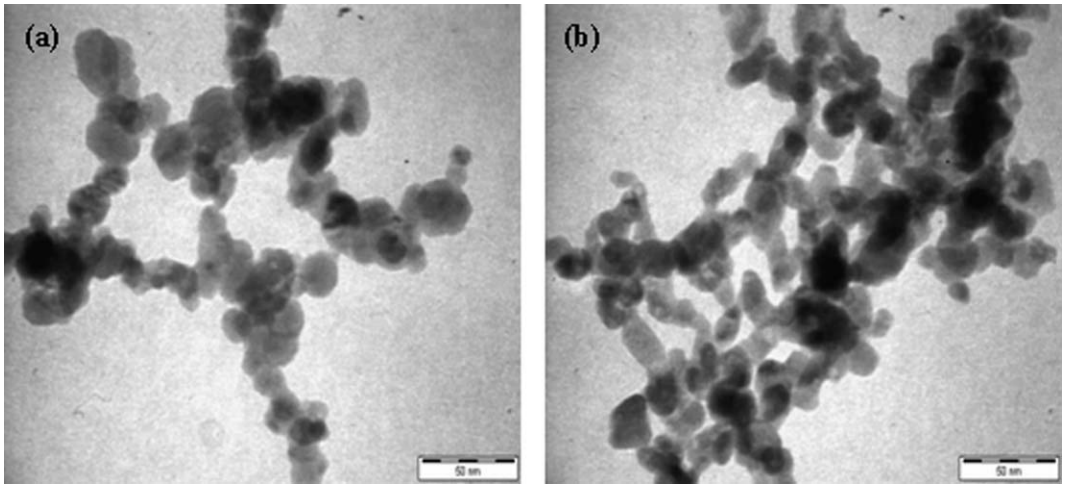

Figure 1 TEM micrographs showing examples of the morphological structures of (a) CuNPs (20 nm) and (b) AgNPs (20 nm) under 500,000× magnification.

RESULTS AND DISCUSSION

Characterization of the nanoparticles

The particle sizes of the nanofillers were measured with the Image Pro Express version 4.0 software on transmission electron microscopy (TEM) images. The TEM images of the AgNPs (20 nm) and CuNPs (20, 50, and 100 nm) were analyzed on the basis of 300 particles. Figure 1 shows examples of the morphological structures of 20-nm CuNPs and AgNPs. Figure 2 shows the particle size distribution of the AgNPs and CuNPs. From the measurements taken, we concluded that the commercial AgNPs and CuNPs had very narrow particle size distributions, where approximately 50% of the nanoparticles fell in the size range.

Electrical conductivity testing

Figure 3 shows the electrical conductivity of various CuNP filler loadings. The morphology of the nanocomposites observed by scanning electron microscopy (SEM) and LM are shown in Figures 4 and 5. In this LM technique, the regions of epoxy matrix and the CuNPs could be easily distinguished. As light from LM passed through the ECA film, the area containing the CuNPs was revealed as a dark brown region, whereas the pure epoxy matrix appeared transparent. The incorporation of CuNPs in the nanocomposite improved the electrical conductivity behavior of the nanocomposite. This improvement was due to the formation of CuNP contacts in the epoxy matrix that allowed electron tunneling in the presence of an electrical current.[2,3,5] As the filler loading increased, more networks of conductive fillers were formed; this allowed more current to flow through,[10–14] as observed by the SEM and LM images in Figure 4. However, the electrical conductivity did not show a significant increase when 3 vol % CuNPs were incorporated because the epoxy was still the dominant phase in the nanocomposite and acted a resistance on electron transmission.

In the context of electrical conductivity, the percolation threshold represents the filler proportion at which the first conduction path is formed.[1] In other words, the percolation threshold is the value of filler content where a further increase of filler loading does not causes significant changes in the electrical conductivity. A statistical model that correlated the relationship between the filler volume fraction and electrical percolation threshold[15,16] was adopted to compare the experimental and theoretical electrical percolation threshold values. The equations of the model are shown in eqs. (1) and (2):

$$V_f < V_p : \sigma_{DC} = \sigma_i (V_p - V_f)^{-s} \quad (1)$$

$$V_f > V_p : \sigma_{DC} = \sigma_f (V_f - V_p)^{t} \quad (2)$$

where V_f is the filler volume fraction, V_p is the percolation threshold volume fraction, σ_{DC} is the conductivity of the composite (S/cm), σ_i is the conductivity of the epoxy matrix, σ_f is the filler conductivity, s is the critical exponent, and t is the critical index of conductivity.

By substituting the experimental value of electrical conductivity into eqs. (1) and (2), values of $t = 3.55$ and $s = 0.64$ were obtained. From Figure 3, we discovered that the experimental percolation threshold occurred at 5 vol %; this was much lower than the theoretical value supposedly occurring at 7 vol %. The shift of the percolation threshold to 5 vol % was

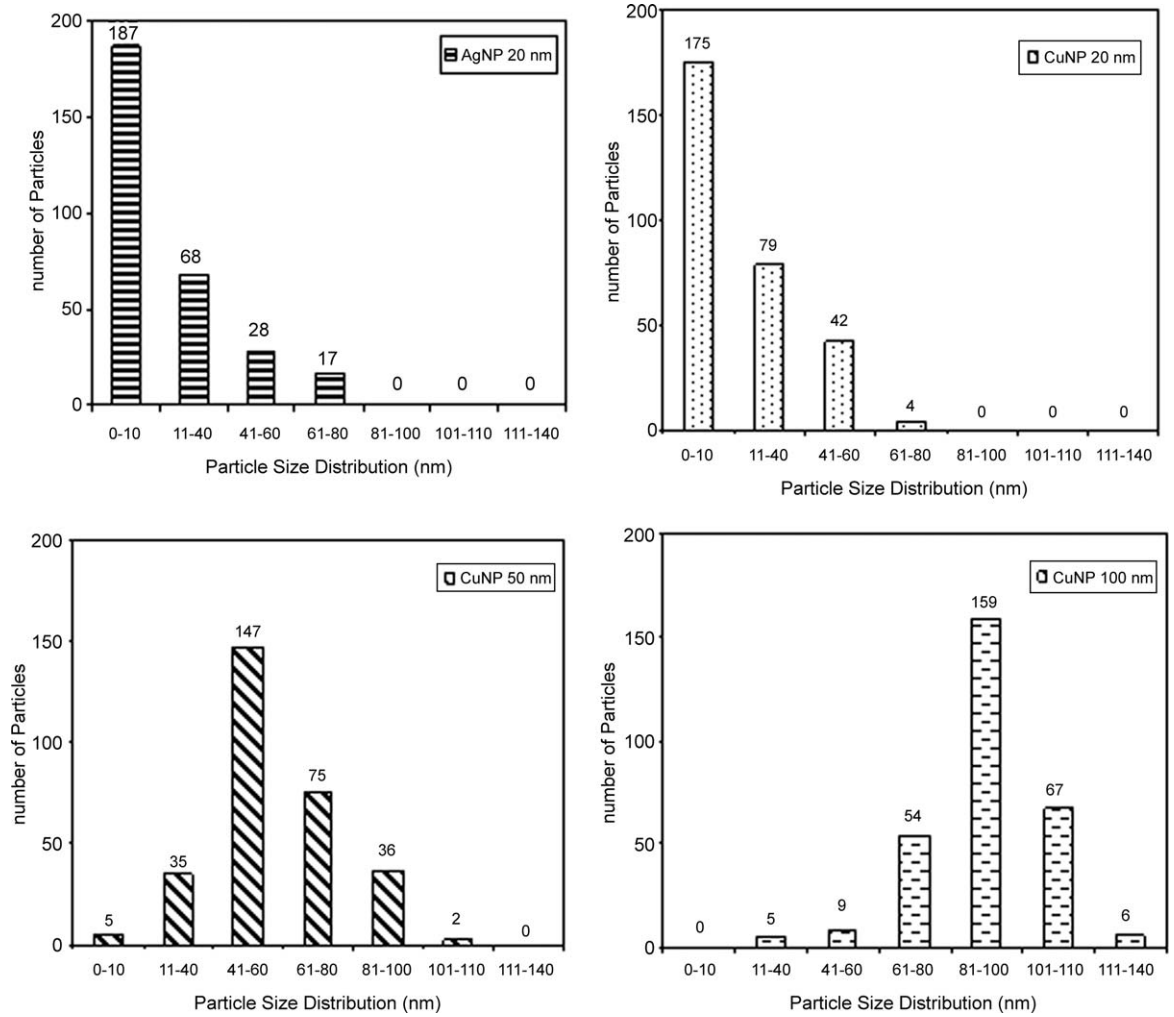

Figure 2 Particle size distribution of AgNPs and CuNPs measured on the basis of TEM images (300 particles were used in the measurement).

due to the agglomeration of the CuNPs in the epoxy matrix; these formed shorter conductive paths to conduct the electric current in the nanocomposites at lower filler loadings.[2]

According to previous studies, the electrical percolation threshold is influenced by the filler size.[12–14] However, in Figure 6, we observed that the electrical percolation threshold for the nanocomposites occurred at 5 vol % regardless of the filler size. Theoretically, smaller fillers result in a higher amount of particles at the same filler content compared to larger particle fillers.[13] Thus, a smaller filler has a higher likelihood of conducting electrons in the filler network; this leads to a higher conductivity.[12,13] However, in reality, this ideal conductive network is not easy to achieve because of the issue of segregation of the nanosized filler, as shown in Figure 4. Attempts at preventing agglomeration with processing techniques were reported in our previous article.[17] Hence, the electrical percolation threshold could only be attained when a higher filler loading (5 vol %) was introduced into the epoxy matrix. After the percolation threshold, the electrical conductivity of the nanocomposites became higher as the particle size decreased. A small-size filler in the epoxy matrix exhibited a higher conductivity because of a higher number of particles at the same filler content compared to larger particle fillers;[13] this subsequently resulted in higher particle-to-particle contact and increased the electrical conductivity. As expected, the electrical conductivity of the nanocomposites loaded with AgNPs was slightly higher than that of the nanocomposites loaded with CuNPs because of the slightly higher electrical conductivity of silver compared to copper. However, the electrical conductivity of the composites also depended on the filler loading, dispersion, and distribution; the aspect ratio of the nanoparticles; the adhesion of nanofiller–matrix; and other factors.[2]

The electrical conductivity results shown in Figure 6 brought important information to our attention in that the electrical conductivity of the

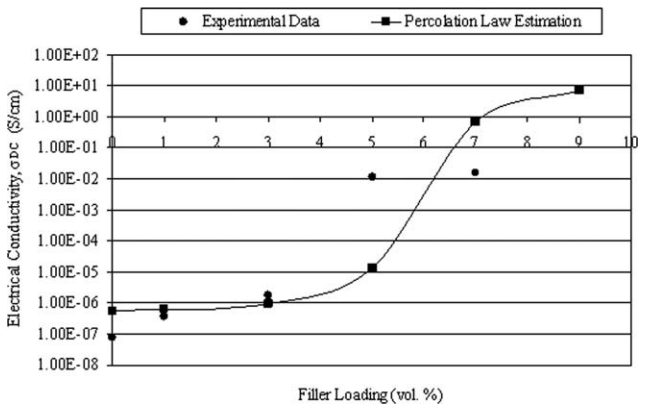

Figure 3 Electrical conductivities of the nanocomposites incorporated with 20-nm CuNPs at filler loadings of 1, 3, 5, and 7 vol %. The theoretical electrical conductivity was estimated with the percolation law with $t = 3.55$, $s = 0.64$, and $V_p = 5$ vol %.

nanocomposites loaded with CuNPs had an equally high conductivity as the AgNPs when they were incorporated into the epoxy matrix.

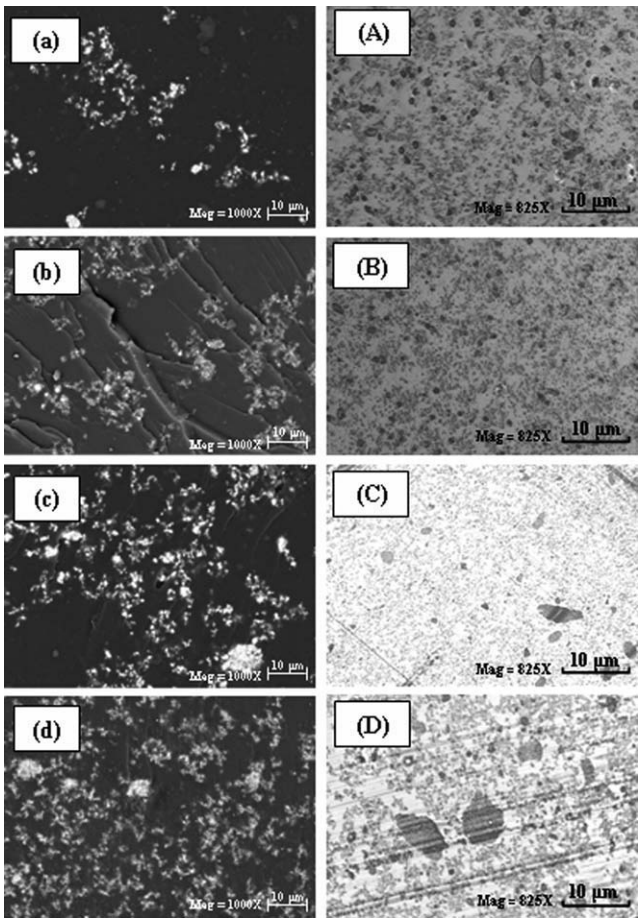

Figure 4 SEM and LM cross-section views of the nanocomposites incorporated with 20-nm CuNPs at various filler loadings: (a/A) 1, (b/B) 3, (c/C) 5, and (d/D) 7 vol % at magnifications of 1000 and 825×, respectively.

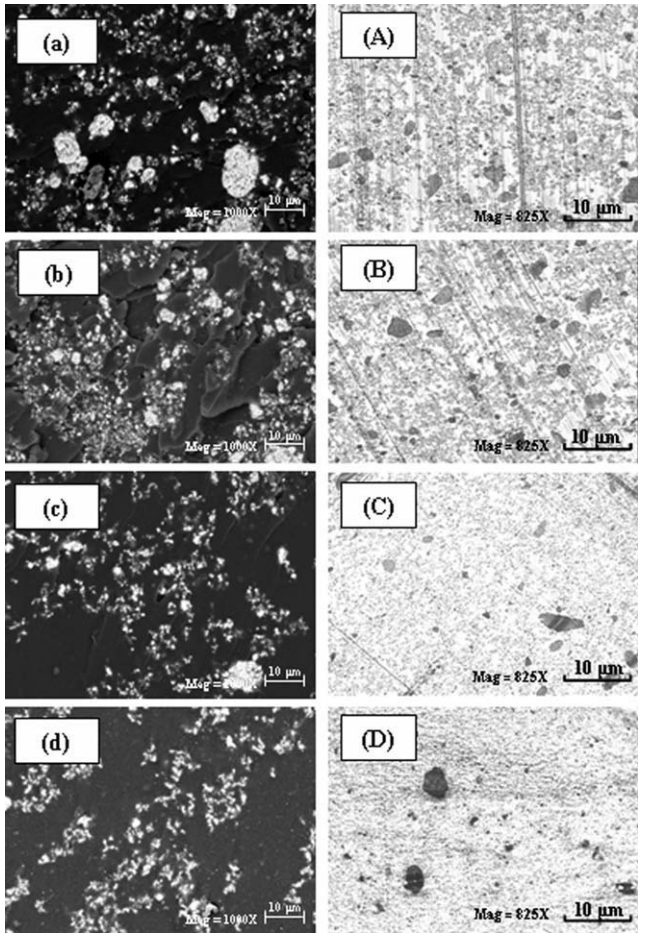

Figure 5 SEM and LM cross-section views of the nanocomposites incorporated with 5 vol % at various filler sizes: (a/A) 100-nm CuNPs, (b/B) 50-mm CuNPs, (c/C) 20-nm CuNPs, and (d/D) 20-nm AgNPs at magnifications of 1000 and 825×, respectively.

Authors of previous works[1,3] have noted that copper is not a favored conductive filler in ECAs because of its poor thermal oxidation behavior during service life. Initiative was taken in this study to compare the effect of thermal aging on the CuNP-

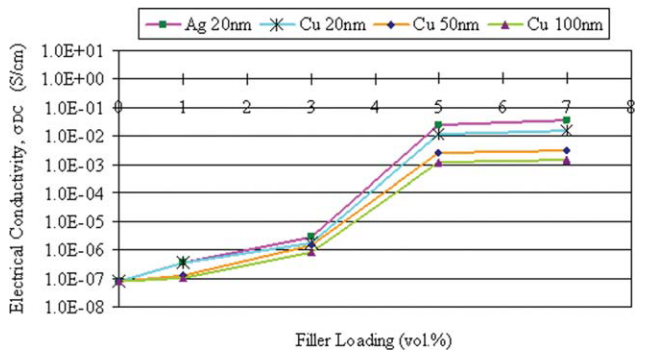

Figure 6 Electrical conductivities of the nanocomposites with various types of filler at filler loadings of 0, 1, 3, 5, and 7 vol %. [Color figure can be viewed in the online issue, which is available at wileyonlinelibrary.com.]

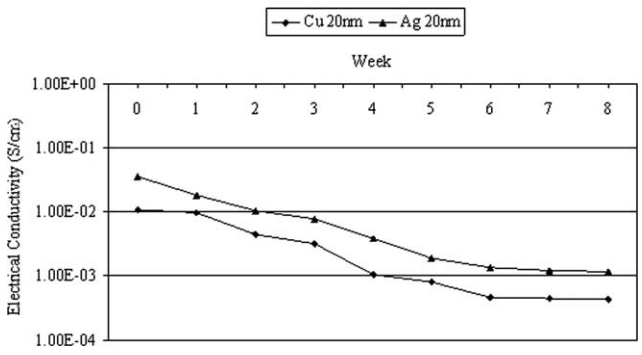

Figure 7 Electrical conductivities of 20-nm CuNP- and AgNP-filled epoxy composites at 5 vol % filler loading and subjected to heat at 150°C for 8 weeks.

and AgNP-filled composites over a period of 8 weeks. As shown in Figure 7, the electrical conductivity of both nanocomposites dropped gradually over the initial 6 weeks and stabilized after an additional 2 weeks of heating. However, the drop in the trend of electrical conductivity in both composite systems was observed to occur at a temperature of 150°C, where a reduction of about one order of magnitude was registered. This test certified that both nanocomposites were stable and suitable for use with ECA in electronic packaging at extremely high temperatures, without significant deterioration of the electrical properties. Notably, the maximum service temperature of electronic packaging was approximately 80°C.

Three-point bending testing

The effects of various filler loadings and filler sizes were characterized, and the flexural modulus and flexural strength values were obtained, as shown in Figures 8 and 9, respectively. As expected, on the basis of the rule of mixtures, the addition of nanoparticles to the epoxy matrix improved the flexural properties of the composite. The flexural modulus increased significantly, approximately 33%, to 4

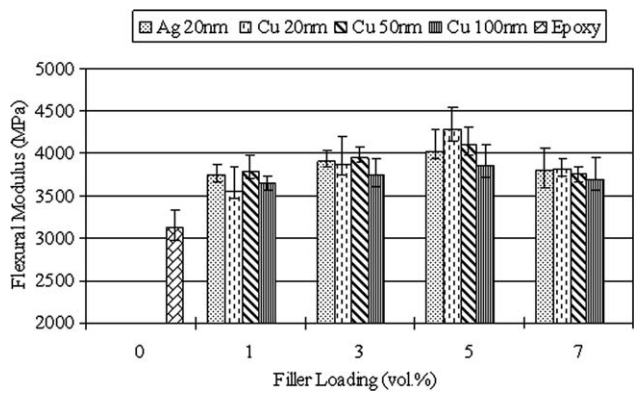

Figure 8 Flexural moduli of the nanocomposites as a function of the filler loading and filler size.

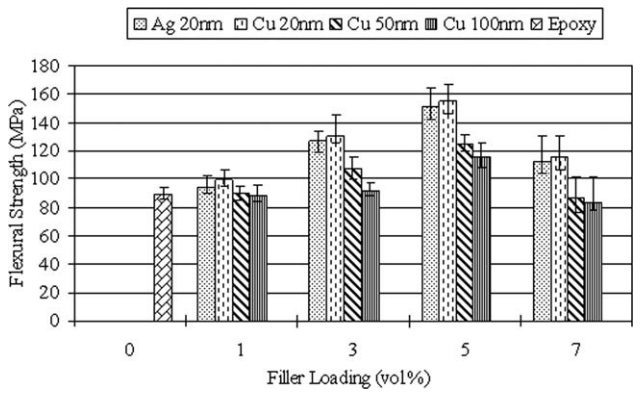

Figure 9 Flexural strengths of the nanocomposites as a function of the filler loading and filler sizes.

GPa, when 5 vol % nanoparticles were added, regardless of the type of filler or filler size. The nanoparticles in the epoxy matrix had a higher stiffness compared to the thermoset epoxy matrix and, thus, acted as a reinforcing agent that aided the material in withstanding the external subjected flexural forces. As the filler content increased from 0 to 5 vol %, a higher portion of reinforcing fillers were present in the epoxy matrix. This filler provided the effect of stiffening the epoxy phase, and thus, the flexural modulus increased proportionally; this was observed in the study done by Chisholm et al.[18] However, a further increase in the filler content to 7 vol % showed a dramatic reduction in the flexural modulus, regardless of the filler type or size. This was due to excess filler loading, which resulted in the formation of more agglomeration in the epoxy matrix, as shown in Figure 4. The presence of agglomerated nanoparticles or particle–particle bonding resulted in a weakly bonded region because of the existence of voids as compared to the epoxy nanoparticle region. Thus, when forces were exerted on the 7 vol % nanocomposite, the nanocomposite failed prematurely because of the presence of more stress concentration points (agglomerated particles) in the matrix.[7,19]

Figure 9 shows the effect of the filler size on the flexural strength. The flexural strength increased with filler loading; this was followed by a reduction in the flexural strength after optimum loading. The finding paralleled the results presented by Chisholm et al.[18] Figure 9 also shows that the nanocomposite loaded with 20-nm filler had a higher flexural strength than those loaded with 50- and 100-nm fillers. This higher flexural strength was due to the fact that the finer particles resulted in a higher amount of particles present in the matrix at the same filler concentration, as shown in Figure 5. The increased number of particles contributed more resistance toward flexural deformation because of the fact that longer crack propagation routes were formed, which

TABLE I
CTE Values of the Nanocomposites Fabricated with Various Filler Sizes and Loadings

Sample	T_g	CTE 1 (ppm/K)	CTE 2 (ppm/K)
Filler loading (20-nm Cu)			
0 vol %	72	95	131
1 vol %	75	81	102
3 vol %	82	69	113
5 vol %	88	57	104
7 vol %	92	43	98
Filler size (5vol %)			
100-nm Cu	85	79	108
50-nm Cu	78	65	105
20-nm Cu	88	57	104
20-nm Ag	89	62	104

CTE 1 and CTE 2 refer to the values of CTE before and after T_g, respectively.

resulted from the higher number of particles. To cause nanocomposite failure, a higher energy or force was required to enable the crack to propagate along the nanocomposites.[19]

CTE

The effects of various filler loadings and filler sizes are shown in Table I. The glass-transition temperature (T_g) was greatly dependent on the filler loading of the nanocomposite, where the value of T_g increased when the amount of filler incorporated into the epoxy matrix increased from 0 to 7 vol %. The enhancement of T_g also indicated that nanofillers could be used as reinforcing fillers to restrict the mobility of the molecular chains in the epoxy. In addition, increasing the filler loading in the nanocomposite reduced the CTE value by approximately 50%, from 95 ppm/K (neat epoxy system) to 43 ppm/K (7 vol %), as shown in Table I. This was due to the increment of filler loading, which resulted in the distribution of more filler over the epoxy matrix; this caused the epoxy–nanoparticle physical interactions to increase.[5] As a result, more heating energy was absorbed by the fillers because of their higher heat capacity, and minimal dimensional changes occurred in the filler phase instead of in the matrix portion.[5] This subsequently caused smaller changes in the nanocomposite dimensions with temperature.

The effect of the filler size was not very significant on the value of T_g. However, the value of CTE 1 (before T_g) was reduced from 79 to 57 ppm/K as the filler size decreased from 100 to 20 nm. Referring to Figure 5, a smaller sized filler had better distribution over the matrix region. Hence, a nanocomposite with smaller particle size had a more homogeneous area of epoxy–filler; this was more effective in restricting the nanocomposite from expansion with temperature.

Thermogravimetric analysis

Table II shows the thermal degradation parameters of the nanocomposites fabricated with various sizes of fillers and filler loadings. All of the nanocomposites had good thermal stability with very low or no weight lost at a temperature of 150°C. This was sufficient for the ECA to serve as a material for electronic packaging because the operating temperature rarely exceeds 100°C. After the burnoff process at 700°C, the residual weight was a good indication for determining the distribution in a quantitative manner, apart from the use of visual aids from SEM and LM techniques. The weight residue information shown in Table II indicated that both low and high filler loadings of fabricated nanocomposites resulted in quite even and good filler distributions in the epoxy matrix.

The onset degradation temperature was higher for nanocomposites with a higher filler loading (7 vol %). A higher filler loading required a higher temperature and energy input to initiate the degradation of the nanocomposite because more fillers were present to dissipate the heating energy away from the epoxy matrix.[5,7]

TABLE II
Thermal Properties of the Nanocomposites Fabricated with Various Filler Sizes and Loadings

Sample	Initial degradation temperature (°C)	Onset degradation temperature (°C)	Weight of residue (%)
Low filler loading (1 vol %)			
Epoxy	354	364	6.5
20-nm Ag	340	347	14.9
20-nm Cu	291	288	11.3
50-nm Cu	288	286	14.1
100-nm Cu	287	287	13.8
High filler loading (7 vol %)			
20-nm Ag	351	358	45.5
20-nm Cu	337	345	38.6
50-nm Cu	330	344	46.8
100-nm Cu	326	346	42.7

Further analysis of the initial and onset degradation temperatures in Table II showed an interesting indication, where the neat epoxy matrix had a high thermal stability followed by the nanocomposites loaded with 20-nm AgNP and 20-nm CuNP. The neat epoxy had the highest thermal stability because of its natural behavior as an insulative material, which resisted energy buildup in the material itself. According to Liufu et al.,[20] degradation occurs initially at the outer surface where the heating energy is bombarded. Eventually, the outer surface gives way for further degradation to occur in the inner structure. This mechanism provides the highest resistance to thermal degradation, and thus, a higher temperature is required to degrade the neat epoxy system. Additionally, the incorporation of CuNPs and AgNPs facilitated thermal degradation in the nanocomposite. In other words, the nanoparticles served as a catalyst to promote thermal degradation by spreading heat energy toward the surrounding epoxy matrix.[7] The nanocomposite incorporated with AgNPs had a higher thermal stability than the nanocomposite loaded with CuNPs. This was because the CuNPs had a higher specific heat capacity, with a value of 0.385 J g^{-1} $°C^{-1}$, than the AgNPs, with a value of 0.234 J g^{-1} $°C^{-1}$. During heating, more energy was absorbed by the CuNPs than the AgNPs and was conducted over the epoxy matrix. Thus, CuNP induced and catalyzed the degradation, which occurred sooner and at a lower temperature than with the AgNPs.

CONCLUSIONS

In conclusion, the results show that optimum overall properties of the nanocomposite were achieved at 5 vol % with the incorporation of 20-nm filler. From the studies, the filler loading had a greater effect on the electrical, mechanical, and thermal properties of the ECA compared to the effect of various filler sizes. Both the CuNP- and AgNP-filled epoxy nanocomposites showed similar thermal resistances over a period of 8 weeks. A drop of one order of magnitude in the electrical conductivity was observed for both nanocomposites, which stabilized after the 6th week at an approximate value of 10^{-3} S/cm. Overall, it we concluded that the electrical, mechanical, and thermal properties of the ECA were slightly similar when 20-nm CuNP or AgNP fillers were incorporated into the epoxy nanocomposite.

References

1. Irfan, M.; Kumar, D. Int J Adhes Adhes 2008, 28, 362.
2. Tee, D. I.; Mariatti, M.; Azizan, A.; See, C. H.; Chong, K. F. Compos Sci Technol 2007, 67, 2584.
3. Li, Y.; Wong, C. P. Mater Sci Eng 2006, R51, 1.
4. Yim, M. J.; Kwon, W. S.; Paik, K. W. Mater Sci Eng B 2006, 126, 59.
5. Lyut, A. S.; Molefi, J. A.; Krump, H. Polym Degrad Stab 2006, 91, 1629.
6. Liang, Y.; Xia, X. H.; Luo, Y. S.; Jia, Z. J. Mater Lett 2007, 61, 3269.
7. Guo, Z. H.; Liang, X. F.; Pereira, T.; Scaffaro, R.; Hann, H. T. Compos Sci Technol 2007, 67, 2036.
8. Wang, Q.; Xia, H. S.; Zhang, C. H. J Appl Polym Sci 2000, 80, 1478.
9. Xia, H. S.; Zhang, C. H.; Wang, Q. J Appl Polym Sci 2000, 80, 1130.
10. Yu, D. M.; Wu, J. S.; Zhou, L. M.; Xie, D. R.; Wu, S. Z. Compos Sci Technol 2000, 60, 499.
11. Psarras, G. C.; Manolakaki, E.; Tsangaris, G. M. Compos A 2003, 34, 1187.
12. Roldughin, V. I.; Vysotskii, V. V. Prog Org Coat 2000, 39, 81.
13. Wu, H. P.; Wu, X. J.; Ge, M. Y.; Zhang, G. Q.; Wang, Y. W.; Jiang, J. Z. Compos Sci Technol 2006, 67, 1116.
14. Wu, H. P.; Liu, J. F.; Wu, X. J.; Ge, M. Y.; Wang, Y. W.; Zhang, G. Q.; Jiang, J. Z. Int J Adhes Adhes 2006, 26, 617.
15. Zhang, M. Q.; Zeng, H. M. In Handbook of Thermoplastics; Olabisi, O., Ed.; Marcel Dekker: New York, 1997; Chapter 35, Vol. 1.
16. Gonon, P.; Boudefel, A. J Appl Phys 2006, 99, 024308.
17. Chan, K. L.; Mariatti, M.; Lockman, Z.; Sim, L. C. J Mater Sci Mater Electron, 2010, 21, 772–778.
18. Chisholm, N.; Mahfuz, H.; Rangari, V. K.; Ashfaq, A.; Jeelani, S. Compos Struct 2005, 67, 115.
19. Frank, H.; Bernd, W. In Polymer Composites: From Nano- to Macro-Scale; Klaus, F., Stoyko, F., Zhang, Z., Eds.; Springer: New York, 2005; Vol. 1.
20. Liufu, S. C.; Xiao, H. N.; Li, Y. P. Polym Degrad Stab 2005, 87, 103.